Full length article

Nonlinear dynamic analysis and vibration of eccentrically stiffened S-FGM elliptical cylindrical shells surrounded on elastic foundations in thermal environments

Nguyen Dinh Duc[a,b,*], Pham Dinh Nguyen[a], Nguyen Dinh Khoa[a]

[a] Advanced Materials and Structures Laboratory, VNU-Hanoi, University of Engineering and Technology (UET), 144, Xuan Thuy, Cau Giay, Hanoi, Vietnam
[b] Infrastructure Engineering Program, VNU-Hanoi, Vietnam-Japan University (VJU), My Dinh 1, Tu Liem, Hanoi, Vietnam

ABSTRACT

Elliptical cylindrical shell is one of shells with special shape. Up to date, there is no publication on vibration and dynamic of functionally graded elliptical cylindrical shells. Therefore, the purpose of the present study is to investigate the nonlinear dynamic response and vibration of imperfect eccentrically stiffness functionally graded elliptical cylindrical shells on elastic foundations using both the classical shell theory (CST) and Airy stress functions method with motion equations using Volmir's assumption. The material properties are assumed to be temperature - dependent and graded in the thickness direction according to a Sigmoid power law distribution (S-FGM). The S-FGM elliptical cylindrical shell with metal-ceramic-metal layers are reinforced by outside metal stiffeners. Both the S-FGM elliptical shell and metal stiffeners are assumed to be in thermal environment and both of them are deformed under temperature simultaneously. Two cases of thermal loading (uniform temperature rise and temperature variation through thickness) are considered. The nonlinear motion equations are solved by Galerkin method and Runge-Kutta method (nonlinear dynamic response, natural frequencies). The effects of geometrical parameters, material properties, elastic foundations Winkler and Pasternak, the nonlinear dynamic analysis and nonlinear vibration of the elliptical cylindrical shells are studied. The some obtained results are validated by comparing with those in the literature.

1. Introduction

Cylindrical shells are frequently used in the manufacturing of aircrafts, missiles, boilers, automobiles, pipelines and some submarine structures. Furthermore, because of the main components of metal and ceramic with physical properties which are changed with the change in thickness, FGM structures have a very high mechanical strength and heat resistance, therefore, vibration and dynamic analysis of FGM cylindrical shells are one of the major issues that many researchers are especially interested in.

Sheng and Wang [1] studied the thermal vibration buckling and dynamic stability of functionally graded cylindrical shells embedded in an elastic medium. Duc considered nonlinear thermal dynamic analysis of eccentrically stiffened S-FGM circular cylindrical shells [2] and eccentrically stiffened piezoelectric S-FGM circular cylindrical shells [3] surrounded on elastic foundations using the higher-order shear deformation shell theory. Ng et al. [4] investigated the dynamic stability analysis of FGM cylindrical shells under periodic axial loading. Bahadori and Najafizadeh [5] presented the free vibration analysis of

two-dimensional functionally graded axisymmetric cylindrical shell on Winkler–Pasternak elastic foundation by first-order shear deformation theory and using Navier-differential quadrature solution methods. Bich and Nguyen [6] proposed the nonlinear vibration of functionally graded circular cylindrical shells based on improved Donnell equations. Shariyat [7] investigated the dynamic buckling of suddenly loaded imperfect hybrid FGM cylindrical shells with temperature-dependent material properties under thermo-electro-mechanical loads. Du et al. [8] considered the nonlinear forced vibration of functionally graded cylindrical thin shells. Sofiyev and Kuruoglu [9,10] investigated the buckling and vibration of shear deformable functionally graded orthotropic cylindrical shells under external pressures and the dynamic instability of three-layered cylindrical shells containing an FGM interlayer. Duc and Thang [11] studied the nonlinear response of imperfect eccentrically stiffened ceramic-metal-ceramic FGM thin circular cylindrical shells surrounded on elastic foundations and subjected to axial compression. Song et al. [12] investigated the active vibration control of CNT-reinforced composite cylindrical shells via piezoelectric patches. Shen [13] studied the large amplitude vibration behavior of

---

a shear deformable FGM cylindrical shell of finite length embedded in a large outer elastic medium and in thermal environments. Kandasamy et al. [14] considered the numerical study on the free vibration and thermal buckling behavior of moderately thick functionally graded structures in thermal environments. Sepiani et al. [15] investigated the free vibration and buckling of a two-layered cylindrical shell made of inner functionally graded and outer isotropic elastic layer, subjected to combined static and periodic axial forces. Kadoli and Ganesan [16] presented the buckling and free vibration analysis of functionally graded cylindrical shells subjected to a temperature-specified boundary condition. Sepiani et al. [17] studied the vibration and buckling analysis of two-layered functionally graded cylindrical shell, considering the effects of transverse shear and rotary inertia. Jafari et al. [18] proposed the nonlinear vibration of functionally graded cylindrical shells embedded with a piezoelectric layer. Mehralian et al. [19] studied the size-dependent formulation of shear deformable functionally graded piezoelectric cylindrical nano shells is developed based on a new modified couple stress theory. In [20], Duc et al. also considered the nonlinear dynamic analysis of Sigmoid functionally graded circular cylindrical shells on elastic foundations using third order shear deformation theory in thermal environments.

Elliptical cylindrical shell which is one of special cylindrical shell forms also attracts the researchers' attention. Yue et al. [21] studied the elliptical crack normal to functionally graded interface of bonded solids. Ganapathi et al. [22] investigated the free flexural vibration behavior of laminated angle-ply elliptical cylindrical shells. Tornabene et al. studied free vibrations of composite oval and elliptic cylinders by the generalized differential quadrature method in [23] and presented dynamic analysis of thick and thin elliptic shell structures made of laminated composite materials in [24]. Khalifa. [25] considered the effects of non-uniform Winkler foundation and non-homogeneity on the free vibration of an orthotropic elliptical cylindrical shell. Gholizadeh et al. [26] investigated the non singular material parameters for arbitrarily elliptical-cylindrical invisibility cloaks. Li el al. [27] studied the prediction of the elastic critical load of submerged elliptical cylindrical shell based on the vibro-acoustic model. Shariati and Rokhi [28] proposed the numerical and experimental investigations on buckling of steel cylindrical shells with elliptical cutout subject to axial compression. Ahmed [29] investigated the buckling behavior of a radially loaded corrugated orthotropic thin-elliptic cylindrical shell on an elastic foundation.

However, there are very few publications about buckling and post buckling as well as vibration of elliptical plates and elliptical cylindrical shells made of FGM materials. In 2005, Patel et al. [30] presented the free vibration characteristics of functionally graded elliptical cylindrical shells using finite element procedure and the higher-order theory including variable transverse displacement through the thickness. In 2013, Zhang [31] proposed the nonlinear bending analysis of FGM elliptical plates resting on two-parameter elastic foundations. Recently, Duc et al. [32] presented on the nonlinear buckling and postbuckling of an eccentrically stiffness S-FGM elliptical cylindrical shells in thermal environment. And according to the authors' knowledge, no paper on dynamic analysis for FGM elliptical cylindrical shells is published so far.

Therefore, this paper set a research objective of researching the nonlinear dynamic response and vibration of an imperfect eccentrically stiffened functionally graded elliptical cylindrical shells in thermal environment. The material properties are assumed to be temperature - dependent and graded in the thickness direction according to a Sigmoid power law distribution in terms of the volume fractions of constituents with metal - ceramic - metal layers (ES-S-FGM shells). One surface of the ES-S-FGM shells is reinforced by outside metal stiffeners. The S-FGM elliptical cylindrical shells are reinforced by longitudinal and transversal stiffeners and surrounded by Winkler and Pasternak type elastic foundations. Both properties of S-FM elliptical cylindrical shells and stiffeners are assumed to be temperature dependent and deformed under temperature simultaneously. The governing equations are estab-
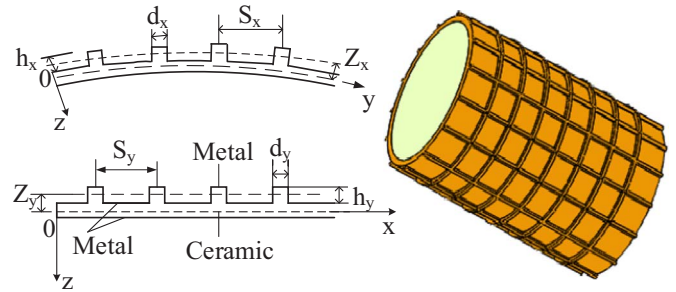

Fig. 1. Geometry and the coordinate system of the functionally graded elliptical cylindrical shells with metal-ceramic-metal layers reinforced by (ES-S-FGM).

lished based on CST theory with motion equations using Volmir's assumptions. The time-amplitude response curves of the cylindrical shell are obtained and the effects of excitation force, elastic foundations, stiffeners, geometrical parameters, material properties, imperfections, mechanical and thermal loads on the vibration and nonlinear dynamic response of ES-S-FGM shells are examined (Fig. 1).

2. Modeling of the ES-S-FGM elliptical cylindrical shells surrounded on elastic foundations

Consider an eccentrically stiffened moderately thin elliptical cylindrical shells with metal-ceramic-metal layers (ES-S-FGM elliptical cylindrical shells). The length, mean radius and total thickness of the shell are L, R and h, respectively. The outside of the ellipse is eccentrically stiffeners in both directions (where s_x, s_y are spacing of the stringer and ring stiffeners, respectively; A_x, A_y are cross-section areas of stiffeners; z_x, z_y are eccentrically of stiffeners with respect to the middle surface the shell; d_x, h_x and d_y, h_y are width and height of the stringer and ring stiffened, respectively) and the inner is placed on the elastic foundations. The shell is defined in a coordinate system (x, θ, z) where x and θ are in the axial and circumferential directions of the shell, respectively, and z is perpendicular to the surface and points outwards $(-h/2 \leq z \leq h/2)$.

2.1. Material properties of the ES-S-FGM shells

Because FGM are typically made from a mixture of metal and ceramic, their material properties are related to both the material properties and the continual distribution of the constituent materials [33–35,37]. Meanwhile, the material properties of both metal and ceramic are related to environmental temperature. Thus, FGM material properties vary smoothly through their thickness and exhibit temperature dependency.

The material properties of the constituent materials P_r (where the subscripts "r" will be replaced with "c" or "m" corresponding to ceramic or metal, respectively) are usually expressed as the following nonlinear function of temperature T [32,38]:

$$P_r(T) = c_0(c_{-1}T^{-1} + 1 + c_1T + c_2T^2 + c_3T^3), \tag{1}$$

in which $T = T_0 + \Delta T$, ΔT is the temperature increment of the environment containing the shell and $T_0 = 300K$ (room temperature), and c_0, c_{-1}, c_1, c_2, c_3 are coefficients characterizing of the constituent materials with temperature-dependent given in Table 1.

The material properties of FGM such as the elastic modulus E, the mass density ρ and the thermal expansion coefficient α are related not only to the material properties of the constituent materials, but also to their volume fraction V_c and V_m:

$$P(z, T) = P_c(T)V_c(z) + P_m(T)V_m(z), \quad V_c + V_m = 1 \tag{2}$$

in which P_c and P_m denotes a material property of ceramic and metal.

For an S-FGM shell made of two different constituent materials with metal-ceramic-metal layers, the volume fractions $V_c(z)$ and $V_m(z)$ can be

Table 1
Temperature – dependent coefficients of the silicon nitride and stainless steel.

Material	Property	c_0	c_{-1}	c_1	c_2	c_3
Si_3N_4 (Ceramic)	$E(Pa)$	384.43×10^9	0	-3.07×10^{-4}	2.16×10^{-7}	-8.946×10^{-11}
	$\rho(kg/m^3)$	2370	0	0	0	0
	$\alpha(K^{-1})$	5.87×10^{-6}	0	9.10×10^{-4}	0	0
	$k(W/mK)$	13.723	0	0	0	0
$SUS304$ (Metal)	$E(Pa)$	201.04×10^9	0	3.08×10^{-4}	-6.534×10^{-7}	0
	$\rho(kg/m^3)$	8166	0	0	0	0
	$\alpha(K^{-1})$	12.33×10^{-6}	0	8.09×10^{-4}	0	0
	$k(W/mK)$	15.379	0	0	0	0

written in the Sigmoid power law distribution (S-FGM) as [11,20].

$$V_c(z) = \begin{cases} \left(1 + \dfrac{2z}{h}\right)^N, & -h/2 \leq z \leq 0 \\ \left(1 - \dfrac{2z}{h}\right)^N, & 0 \leq z \leq h/2 \end{cases} \tag{3}$$

where N is power law exponent satisfying $0 \leq N < \infty$. Using Eqs. (2) and (3), the material properties of S-FGM are written as

$$P(z, T) = \begin{cases} (P_c(z, T) - P_m(z, T))\left(1 + \dfrac{2z}{h}\right)^N + P_m(z, T), & -\dfrac{h}{2} \leq z \leq 0 \\ (P_c(z, T) - P_m(z, T))\left(1 - \dfrac{2z}{h}\right)^N + P_m(z, T), & 0 \leq z \leq \dfrac{h}{2} \end{cases} \tag{4}$$

Accordingly, the effective Young's modulus $E(z, T)$, thermal expansion coefficient $\alpha(z, T)$, the mass density $\rho(z, T)$ and coefficient of thermal conduction K of S-FGM structures can be written in the similar form of Eq. (4).

$$[E(z, T), \alpha(z, T), \rho(z, T), K(z, T)] = [E_m(z, T), \alpha_m(z, T),$$
$$\rho_m(z, T), K_m(T)]$$
$$+[E_{cm}(z, T), \alpha_{cm}(z, T), \rho_{cm}(z, T), K_{cm}(z, T)] \begin{cases} \left(1 + \dfrac{2z}{h}\right)^N, & -\dfrac{h}{2} \leq z \leq 0 \\ \left(1 - \dfrac{2z}{h}\right)^N, & 0 \leq z \leq \dfrac{h}{2} \end{cases} \tag{5}$$

where $E_{cm}(z, T) = E_c(z, T) - E_m(z, T)$, $\alpha_{cm}(z, T) = \alpha_c(z, T) - \alpha_m(z, T)$ $\rho_{cm}(z, T) = \rho_c(z, T) - \rho_m(z, T)$ and $K_{cm}(z, T) = K_c(z, T) - K_m(z, T)$. The Poisson's ratio v is assumed constant, $v(z, T) = v$.

2.2. Elastic foundations

The ES-S-FGM elliptical cylindrical shells surrounded on elastic foundations (Fig. 2). The reaction–deflection relation of Pasternak foundation is given by:

$$q_e = k_1 w - k_2 \nabla^2 w \tag{6}$$

where $\nabla^2 = \dfrac{\partial^2}{\partial x^2} + \dfrac{\partial^2}{\partial y^2}$, w is the deflection of the FGM shell, k_1 and k_2 are Winkler foundation stiffness and shear layer stiffness of Pasternak foundation, respectively.

In Fig. 2, R - the principal radii of curvature in the circumferential direction, which depends on the type of cross-section. For elliptical cross-section, R can be described as [30,32]:

$$R = (b^2/R_0)(1 + \mu_0 \cos 2\theta)^{-3/2} \tag{7}$$

in which both R_0 and μ_0 as follows:

$$R_0 = [(a^2 + b^2)/2]^{\frac{1}{2}}, \quad \mu_0 = [(a^2 - b^2)/(a^2 + b^2)]; \tag{8}$$

where a, b are the lengths of semi-major and semi-minor axes of elliptical cross-section.

3. Governing equations and boundary conditions

3.1. Governing equation for ES-S-FGM shells

In this study, the CST is used to establish the governing equations and determine the nonlinear response of the ES-S-FGM thin elliptical cylindrical shells, taking into account thermal deformation of both the shells as well as stiffeners.

For the elliptical cylindrical shells, the nonlinear strain-displacement relations on the middle surface using CST are [37–40]:

$$\begin{Bmatrix} \varepsilon_x \\ \varepsilon_y \\ \gamma_{xy} \end{Bmatrix} = \begin{Bmatrix} \varepsilon_x^0 \\ \varepsilon_y^0 \\ \gamma_{xy}^0 \end{Bmatrix} + z \begin{Bmatrix} k_x \\ k_y \\ k_{xy} \end{Bmatrix} = \begin{Bmatrix} \dfrac{\partial u}{\partial x} + \dfrac{1}{2}\left(\dfrac{\partial w}{\partial x}\right)^2 \\ \dfrac{\partial v}{\partial y} - \dfrac{w}{R} + \dfrac{1}{2}\left(\dfrac{\partial w}{\partial y}\right)^2 \\ \dfrac{\partial u}{\partial y} + \dfrac{\partial v}{\partial x} + \dfrac{\partial w}{\partial x}\dfrac{\partial w}{\partial y} \end{Bmatrix} - z \begin{Bmatrix} \dfrac{\partial^2 w}{\partial x^2} \\ \dfrac{\partial^2 w}{\partial y^2} \\ 2\dfrac{\partial^2 w}{\partial x \partial y} \end{Bmatrix} \tag{9}$$

where ε_x^0, ε_y^0 and γ_{xy}^0 are the strain components on the reference surface. $u(x, y, t)$, $v(x, y, t)$ and $w(x, y, t)$ are the displacements along x, y and z axes, respectively.

Hooke's law for the ES-S-FGM elliptical cylindrical shells can be defined as [11,20,32,37]:

$$\sigma_x = K(z, T)\{\varepsilon_x + v\varepsilon_y - (1 + v)\alpha\Delta T\},$$
$$\sigma_y = K(z, T)\{\varepsilon_y + v\varepsilon_x - (1 + v)\alpha\Delta T\}$$
$$\sigma_{xy} = \dfrac{1}{2}K(z, T)(1 - v)\gamma_{xy}, \tag{10}$$

where $K(z, T) = E(z, T)/(1 - v^2)$

In order to provide continuity between the shell (with metal-ceramic-metal layers) and stiffeners, suppose that stiffeners are made of full metal. For stiffeners in thermal environments with temperature-dependent properties, we have proposed its form be adopted from [11,20,32,37], as follows

$$\sigma_x^s = E^s\varepsilon_x - \dfrac{E^s}{1 - 2v^s}\alpha^s\Delta T$$
$$\sigma_y^s = E^s\varepsilon_y - \dfrac{E^s}{1 - 2v^s}\alpha^s\Delta T \tag{11}$$

in which, $E^s = E_m$, $v^s = v_m$, $\alpha^s = \alpha_m$, are Young's modulus, Poisson's ratio and thermal expansion coefficient of the stiffeners, respectively.

The force and moment resultants of the ES-S-FGM elliptical cylindrical shells are shown in a new form as:
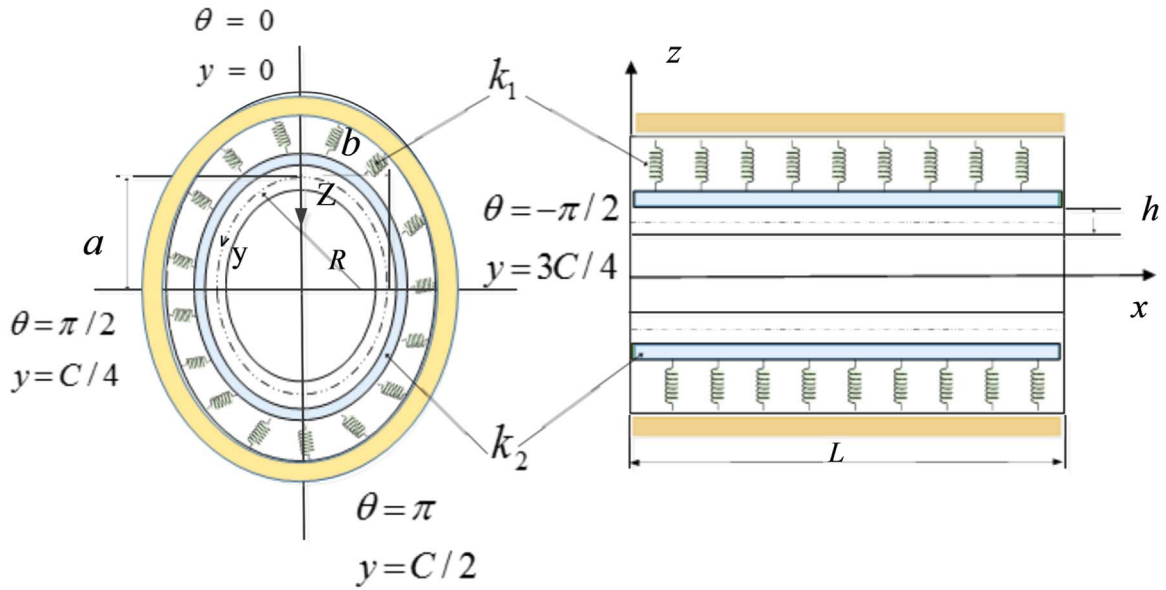
Fig. 2. Geometry and coordinate system of the ES-S-FGM elliptical cylindrical shells surrounded on elastic foundations.

$$N_x = \int_{-h/2}^{h/2} \sigma_x dz + \frac{1}{s_x} \int_{A_x} \sigma_x^s dA_x, \quad N_y = \int_{-h/2}^{h/2} \sigma_y dz + \frac{1}{s_y} \int_{A_y} \sigma_y^s dA_y,$$

$$N_{xy} = \int_{-h/2}^{h/2} \sigma_{xy} dz$$

$$M_x = \int_{-h/2}^{h/2} \sigma_x z dz + \frac{1}{s_x} \int_{A_x} \sigma_x^s z dA_x, \quad M_y = \int_{-h/2}^{h/2} \sigma_y z dz + \frac{1}{s_y} \int_{A_y} \sigma_y^s z dA_y,$$

$$M_{xy} = \int_{-h/2}^{h/2} \sigma_{xy} z dz$$

$$(12)$$

Substitution Eq. (9) into Eqs. (10), (11) and results into (12) yields the constitutive relations as:

$$\begin{Bmatrix} N_x \\ N_y \\ N_{xy} \\ M_x \\ M_y \\ M_{xy} \end{Bmatrix} = \begin{bmatrix} A_{11} & A_{12} & 0 & B_{11} & B_{12} & 0 \\ A_{12} & A_{22} & 0 & B_{12} & B_{22} & 0 \\ 0 & 0 & A_{66} & 0 & 0 & B_{66} \\ B_{11} & B_{12} & 0 & D_{11} & D_{12} & 0 \\ B_{12} & B_{22} & 0 & D_{12} & D_{22} & 0 \\ 0 & 0 & B_{66} & 0 & 0 & D_{66} \end{bmatrix} \begin{Bmatrix} \varepsilon_x^0 \\ \varepsilon_y^0 \\ \gamma_{xy}^0 \\ k_x \\ k_y \\ k_{xy} \end{Bmatrix} - \begin{Bmatrix} \Phi_1 + \Phi_{1x}^s \\ \Phi_1 + \Phi_{1y}^s \\ 0 \\ \Phi_1 + \Phi_{2x}^s \\ \Phi_1 + \Phi_{2y}^s \\ 0 \end{Bmatrix}$$

$$(13a)$$

$$(\Phi_1, \Phi_2) = \frac{1}{1-v} \int_{-h/2}^{0} E_{(z)} \alpha_{(z)} \Delta T_{(z)} (1, z) \, dz + \frac{1}{1-v} \int_{0}^{h/2} E_{(z)} \alpha_{(z)} \Delta T_{(z)} (1, z) \, dz,$$

$$(\Phi_{1i}^s, \Phi_{2i}^s) = \frac{1}{1-2v} \int_{h/2}^{h/2+h_i} E^s \alpha_s \Delta T_s (1, z) \frac{d_i^T}{s_i^T} dz, \quad i = x, y$$

$$(13b)$$

where $A_{ij}, B_{ij}, D_{ij} (i = 1 \div 6, j = 1 \div 6)$ are given in Appendix A.

After the thermal deformation process, the geometric shapes of stiffeners which can be determined as [11,20,32,37]:

$$d_x^T = d_x [1 + a_m \Delta T(z)], \quad d_y^T = d_y [1 + a_m \Delta T(z)]$$
$$h_x^T = h_x [1 + a_m \Delta T(z)], \quad h_y^T = h_y [1 + a_m \Delta T(z)]$$
$$z_x^T = z_x [1 + a_m \Delta T(z)], \quad z_y^T = z_y [1 + a_m \Delta T(z)]$$
$$s_x^T = s_x [1 + a_m \Delta T(z)], \quad s_y^T = s_y [1 + a_m \Delta T(z)]$$

$$(14)$$

The nonlinear motion equations of the ES-S-FGM elliptical cylindrical shells surrounded on elastic foundations using CST are [37–40]:

$$\frac{\partial N_x}{\partial x} + \frac{\partial N_{xy}}{\partial y} = \rho_1 \frac{\partial^2 u}{\partial t^2},$$

$$(15a)$$

$$\frac{\partial N_{xy}}{\partial x} + \frac{\partial N_y}{\partial y} = \rho_1 \frac{\partial^2 v}{\partial t^2},$$

$$(15b)$$

$$\frac{\partial^2 M_x}{\partial x^2} + 2 \frac{\partial^2 M_{xy}}{\partial y^2} + \frac{\partial^2 M_y}{\partial y^2} + N_x \frac{\partial^2 w}{\partial x^2} + 2 N_{xy} \frac{\partial^2 w}{\partial x \partial y} + N_y \frac{\partial^2 w}{\partial y^2} + p - k_1 w +$$
$$k_2 \left(\frac{\partial^2 w}{\partial x^2} + \frac{\partial^2 w}{\partial y^2} \right) + \frac{N_y}{R} = \rho_1 \frac{\partial^2 w}{\partial t^2}.$$

$$(15c)$$

where $p(Pa)$ is an external pressure uniformly distributed on the surface of the shell.

and

$$\rho_1 = \int_{-\frac{h}{2}}^{\frac{h}{2}} \rho(z, T) dz,$$

$$(16)$$

The Airy stress function $f(x, y, t)$ is introduced as:

$$N_x = \frac{\partial^2 f}{\partial y^2}, \quad N_y = \frac{\partial^2 f}{\partial x^2}, \quad N_{xy} = -\frac{\partial^2 f}{\partial x \partial y}.$$

$$(17)$$

The reverse relations are obtained from Eq. (13a), one can write:

$$\varepsilon_x^0 = A_{22}^* \frac{\partial^2 f}{\partial y^2} - A_{12}^* \frac{\partial^2 f}{\partial x^2} + B_{11}^* \frac{\partial^2 w}{\partial x^2} + B_{12}^* \frac{\partial^2 w}{\partial y^2} + (A_{12}^* - A_{22}^*) \Phi_1 + A_{22}^* \Phi_{1x}^s$$
$$- A_{12}^* \Phi_{1y}^s,$$

$$\varepsilon_y^0 = A_{11}^* \frac{\partial^2 f}{\partial x^2} - A_{12}^* \frac{\partial^2 f}{\partial y^2} + B_{21}^* \frac{\partial^2 w}{\partial x^2} + B_{22}^* \frac{\partial^2 w}{\partial y^2} + (A_{11}^* - A_{12}^*) \Phi_1 - A_{12}^* \Phi_{1x}^s$$
$$+ A_{11}^* \Phi_{1y}^s,$$

$$\gamma_{xy}^0 = -A_{66}^* \frac{\partial^2 f}{\partial x \partial y} + 2 B_{66}^* \left(\frac{\partial^2 w}{\partial x \partial y} \right)$$

$$(18)$$

where
$$A_{11}^* = \frac{A_{11}}{\Delta}, \quad A_{22}^* = \frac{A_{22}}{\Delta}, \quad A_{12}^* = \frac{A_{12}}{\Delta}, \quad A_{66}^* = \frac{1}{A_{66}}, \quad B_{66}^* = \frac{B_{66}}{A_{66}}, \quad \Delta = A_{11}A_{22} - A_{12}^2$$
$$B_{11}^* = A_{22}^* B_{11} - A_{12}^* B_{12}, \quad B_{22}^* = A_{11}^* B_{22} - A_{12}^* B_{12}, \quad B_{12}^* = A_{22}^* B_{12} - A_{12}^* B_{22},$$
$$B_{21}^* = A_{11}^* B_{12} - A_{12}^* B_{11}$$

The nonlinear motion equation of the ES-S-FGM using the Volmir's assumption [36,37]: $u << w, v << w, \rho_1 \frac{\partial^2 u}{\partial t^2} \to 0, \rho_1 \frac{\partial^2 v}{\partial t^2} \to 0$ leads to:

$$\frac{\partial N_x}{\partial x} + \frac{\partial N_{xy}}{\partial y} = 0,$$

$$(19a)$$

$$\frac{\partial N_{xy}}{\partial x} + \frac{\partial N_y}{\partial y} = 0, \tag{19b}$$

$$\frac{\partial^2 M_x}{\partial x^2} + 2\frac{\partial^2 M_{xy}}{\partial y^2} + \frac{\partial^2 M_y}{\partial y^2} + N_x\frac{\partial^2 w}{\partial x^2} + 2N_{xy}\frac{\partial^2 w}{\partial x \partial y} + N_y\frac{\partial^2 w}{\partial y^2} + p - k_1 w +$$

$$k_2\left(\frac{\partial^2 w}{\partial x^2} + \frac{\partial^2 w}{\partial y^2}\right) + \frac{N_y}{R} = \rho_1\frac{\partial^2 w}{\partial t^2}. \tag{19c}$$

The deformation compatibility equation for an imperfect ES-S-FGM can be written as [37,38]:

$$\frac{\partial^2 \varepsilon_x^0}{\partial y^2} + \frac{\partial^2 \varepsilon_y^0}{\partial x^2} - \frac{\partial^2 \gamma_{xy}^0}{\partial x \partial y} =$$

$$\frac{\partial^2 w}{\partial x \partial y} - \frac{\partial^2 w}{\partial x^2}\frac{\partial^2 w}{\partial y^2} + 2\frac{\partial^2 w}{\partial x \partial y}\frac{\partial^2 w^*}{\partial x \partial y} - \frac{\partial^2 w}{\partial x^2}\frac{\partial^2 w^*}{\partial y^2} - \frac{\partial^2 w}{\partial y^2}\frac{\partial^2 w^*}{\partial x^2} - \frac{1}{R}\frac{\partial^2 w}{\partial x^2} \tag{20}$$

in which the imperfection function $w^*(x, y)$ denotes an initial small imperfection of the ES-S- FGM shells.

Substitution Eq. (20) into Eq. (13a) result into Eq. (19c) leads to:

$$B_{21}^*\frac{\partial^4 f}{\partial x^4} + B_{12}^*\frac{\partial^4 f}{\partial y^4} + (B_{11}^* + B_{22}^* - 2B_{66}^*)\frac{\partial^4 f}{\partial x^2 \partial y^2} - C_{11}^*\frac{\partial^4 w}{\partial x^4} - C_{22}^*\frac{\partial^4 w}{\partial y^4}$$

$$+ \frac{1}{R}\frac{\partial^2 f}{\partial x^2} + \frac{\partial^2 f}{\partial y^2}\left(\frac{\partial^2 w}{\partial x^2} + \frac{\partial^2 w^*}{\partial x^2}\right) - (C_{12}^* + C_{21}^* + 4C_{66}^*)\frac{\partial^4 w}{\partial x^2 \partial y^2}$$

$$- 2\frac{\partial^2 f}{\partial x \partial y}\left(\frac{\partial^2 w}{\partial x \partial y} + \frac{\partial^2 w^*}{\partial x \partial y}\right) + \frac{\partial^2 f}{\partial x^2}\left(\frac{\partial^2 w}{\partial y^2} + \frac{\partial^2 w^*}{\partial y^2}\right)$$

$$+ p - k_1 + k_2\nabla^2 w = \rho_1\frac{\partial^2 w}{\partial t^2}. \tag{21}$$

where:

$$C_{11}^* = D_{11} - B_{11}^*B_{11} - B_{21}^*B_{12}, \quad C_{22}^* = D_{22} - B_{12}^*B_{12} - B_{22}^*B_{22},$$
$$C_{12}^* = D_{12} - B_{12}^*B_{11} - B_{22}^*B_{12}, \quad C_{21}^* = D_{12} - B_{11}^*B_{12} - B_{21}^*B_{22},$$
$$C_{66}^* = D_{66} - B_{66}^*B_{66};$$

Replacing Eq. (18) into Eq. (20) leads to:

$$A_{11}^*\frac{\partial^4 f}{\partial x^4} + A_{22}^*\frac{\partial^4 f}{\partial y^4} + (A_{66}^* - 2A_{12}^*)\frac{\partial^4 f}{\partial x^2 \partial y^2} + B_{11}^*\frac{\partial^4 w}{\partial x^4} + B_{12}^*\frac{\partial^4 w}{\partial y^4}$$

$$+ (B_{11}^* + B_{22}^* - 2B_{66}^*)\frac{\partial^4 w}{\partial x^2 \partial y^2}$$

$$- \left(\frac{\partial^2 w}{\partial x \partial y} - \frac{\partial^2 w}{\partial x^2}\frac{\partial^2 w}{\partial y^2} + 2\frac{\partial^2 w}{\partial x \partial y}\frac{\partial^2 w^*}{\partial x \partial y} - \frac{\partial^2 w}{\partial x^2}\frac{\partial^2 w^*}{\partial y^2} - \frac{\partial^2 w}{\partial y^2}\frac{\partial^2 w^*}{\partial x^2} - \frac{1}{R}\frac{\partial^2 w}{\partial x^2}\right)$$

$$= 0; \tag{22}$$

Eqs. (21) and (22) are nonlinear equations in terms of variables w and f and used to investigate the nonlinear vibration and dynamic stability of imperfect ES-S-FGM elliptical cylindrical shells on elastic foundations subjected to mechanical and thermal loads.

3.2. Boundary conditions

In this paper, the edges of ES-S-FGM shells are assumed to be simply supported. Depending on the in-plane restraint at the edges, two cases of boundary conditions, labeled as Case 1 and Case 2 may be considered.

Case 1. Four edges are simply supported and freely movable (FM). The associated boundary conditions are:

$$w = M_x = N_{xy} = 0, \quad N_x = N_{x0} \text{ at } x = 0 \text{ and } x = L \tag{23}$$

Case 2. Four edges are simply supported and immovable (IM). The associated boundary conditions are:

$$w = u = M_x = 0, \quad N_x = N_{x0} \text{ at } x = 0 \text{ and } x = L \tag{24}$$

where N_{x0} are pre-buckling compressive force resultant in direction x.

4. Solutions of the problem

To solve two Eqs. (21) and (22) for unknowns w and f, and with the consideration of the boundary conditions (23) and (24), we assume the following approximate solutions

$$w(x, y, t) = W(t)\sin \lambda_m x \sin \delta_n y$$
$$w^*(x, y, t) = \mu h \sin \lambda_m x \sin \delta_n y$$

$$f(x, y, t) = A_1\cos 2\lambda_m x + A_2\cos 2\delta_n y + A_3\sin \lambda_m x \sin \delta_n y + \frac{1}{2}N_{x0}y^2 \tag{25}$$

where $\lambda_m = m\pi/L$, $\delta_n = n/R$, W is amplitude of the deflection and μ is parameter of imperfection; m, n are odd natural numbers. The coefficients A_i $(i = 1 \div 3)$ are determined by substitution of Eq. (25) into Eq. (18) as:

$$A_1 = B_1 W(W + 2\mu h), \quad A_2 = B_2 W(W + 2\mu h), \quad A_3 = (B_3 + B_4)W \tag{26}$$

where:

$$B_1 = \frac{\delta_n^2}{32A_{11}^*\lambda_m^2}, \quad B_2 = \frac{\lambda_m^2}{32A_{22}^*\delta_n^2},$$

$$B_3 = \frac{\lambda_m^2}{R[A_{11}^*\lambda_m^4 - (2A_{12}^* - A_{66}^*)\lambda_m^2\delta_n^2 + A_{22}^*\delta_n^4]}$$

$$B_4 = -\frac{[B_{21}^*\lambda_m^4 + (B_{11}^* + B_{22}^* - 2B_{66}^*)\lambda_m^2\delta_n^2 + B_{12}^*\delta_n^4]}{[A_{11}^*\lambda_m^4 - (2A_{12}^* - A_{66}^*)\lambda_m^2\delta_n^2 + A_{22}^*\delta_n^4]} \tag{27}$$

Substitution of Eqs. (25) and (26) and (27) into Eq. (19) and applying the Galerkin procedure for resulting equation yield:

$$h_{11}W + h_{12}W(W + \mu h) + h_{13}W(W + 2\mu h) + h_{14}W(W + \mu h)(W + 2\mu h)$$

$$- N_{x0}\lambda_m^4\frac{LR}{4}(W + \mu h) + \frac{4}{\lambda_m\delta_n}p = \rho_1\frac{LR}{4}\frac{\partial^2 W}{\partial t^2}. \tag{28}$$

where the coefficients $h_{ij}(i = 1, j = 1 \div 4)$ are shown in Appendix B.

4.1. Nonlinear dynamic analysis of ES-S-FGM subjected to mechanical load

Consider the ES-S-FGM elliptical cylindrical shells is simply supported and freely movable (FM - Case 1 of boundary conditions), subjected to axial compressive load $N_{x0} = -P_x h$ in which P_x is the average axial stress on the shell's end sections positive when the shells subjected to axial compression. Eq. (28) can be written as following:

$$h_{11}W + h_{12}W(W + \mu h) + h_{13}W(W + 2\mu h) + h_{14}W(W + \mu h)(W + 2\mu h)$$

$$+ P_x\lambda_m^4\frac{LR}{4}h(W + \mu h) + \frac{4}{\lambda_m\delta_n}p = \rho_1\frac{LR}{4}\frac{\partial^2 W}{\partial t^2}. \tag{29}$$

4.2. Nonlinear dynamic analysis of ES-S- FGM with effect of temperature dependent

A simply supported the imperfect ES-S-FGM elliptical cylindrical shells with four edges are simply supported and immovable (IM, Case 2 of boundary conditions) under simultaneous action of uniform external pressure p and under steadily increasing temperature is considered. The condition expressing the immovability on the boundary edges of the shell, i.e, $u = 0$ at $x = 0, L$ is justified in an average sense as [11,20,32,37]:

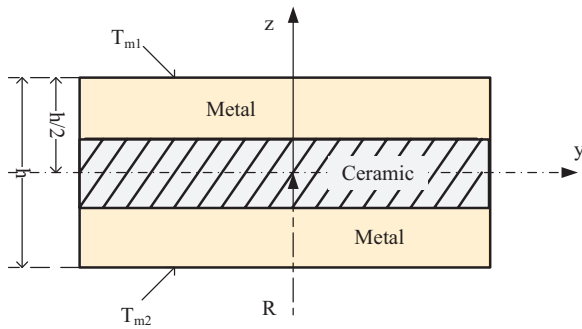$$\int_0^{2\pi R}\int_0^L \frac{\partial u}{\partial x} dx dy = 0 \tag{30}$$

Fig. 3. The temperature variation through ES-S-FGM shell thickness.

From Eq. (9) one can obtain the following expression in which Eq. (18) and imperfect have been included:

$$\frac{\partial u}{\partial x} = A_{22}^* \frac{\partial^2 f}{\partial y^2} - A_{12}^* \frac{\partial^2 f}{\partial x^2} + B_{11}^* \frac{\partial^2 w}{\partial x^2} + B_{12}^* \frac{\partial^2 w}{\partial y^2} + (A_{22}^* - A_{12}^*)\Phi_1 + A_{22}^* \Phi_{1x}^s$$
$$- A_{12}^* \Phi_{1y}^s - \frac{1}{2}\frac{\partial^2 w}{\partial x^2} - \frac{\partial w}{\partial x}\frac{\partial w^*}{\partial x}$$

(31)

Substitution Eq. (25) into (31) and then results into Eq. (30), yield:

$$N_{x0} = \frac{\lambda_m^2}{8A_{22}^*}W(W + 2\mu h) + \frac{A_{22}^* - A_{12}^*}{A_{22}^*}\Phi_1 + \Phi_{1x}^s - \frac{A_{12}^*}{A_{22}^*}\Phi_{1y}^s$$

(32)

4.2.1. Uniform temperature rise

The ES-S-FGM elliptical cylindrical shells is assumed to expose to environment temperature uniformly raised from stress free initial value T_i to final value T_f and temperature change $\Delta T = T_f - T_i$ is independent from thickness variable. The thermal parameter Φ_1 can be expressed in terms of the ΔT as:

$$\Phi_1 = \frac{Ph\Delta T}{1 - v}, \Delta T = const, P = E_m\alpha_m + \frac{E_m\alpha_{cm} + E_{cm}\alpha_m}{N + 1} + \frac{E_{cm}\alpha_{cm}}{2N + 1}$$

(33)

4.2.2. Through the thickness temperature gradient

In this case, the temperature gradient is assumed to vary through the thickness of the ES-S-FGM shell. The metal-rich top surface temperature T_{m1} is maintained at stress free initial value and metal-rich bottom surface temperature T_{m2} is elevated, which are shown in the Fig. 3.

The temperature conduction is governed by one-dimensional Fourier equation as:

$$\frac{d}{d\bar{z}}\left[K(\bar{z})\frac{dT}{d\bar{z}}\right] + \frac{K(\bar{z})dT}{\bar{z}d\bar{z}} = 0$$
$$T|_{z=R-\frac{h}{2}} = T_{m2}, \ T|_{z=R+\frac{h}{2}} = T_{m1}, \ T|_{\bar{z}=R} = T_c; \ \Delta T = T_{m1} - T_{m2}$$

(34)

where $\bar{z}$ the distance from a point which distance is radial coordinate of a point which is distant z from the shell middle surface with respect to the center of the shell, $\bar{z} = R + z$, $(R - \frac{h}{2} \leq \bar{z} \leq R + \frac{h}{2})$.

The solution of Eq. (34) can be obtained as follows:

$$T(\bar{z}) = T_{m2} + \frac{\Delta T}{\int_{R-\frac{h}{2}}^{R+\frac{h}{2}} \frac{d\bar{z}}{\bar{z}K(\bar{z})}}\int_{R-\frac{h}{2}}^{z}\frac{d\zeta}{\zeta K(\zeta)}$$

(35)

This section only considers linear distribution of metal and ceramic constituents, i.e. N=1, the coefficient of thermal conduction K of S-FGM in Eq. (5) leads:

$$K(\bar{z}) = K_m + K_{cm}\begin{cases} \frac{2\bar{z}+h}{h} \ , \ R - \frac{h}{2} \leq \bar{z} \leq R \\ \frac{-2\bar{z}+h}{h}, \ R \leq \bar{z} \leq R + \frac{h}{2}\end{cases}$$

(36)

$$I_1 = \int_{R-\frac{h}{2}}^{R+\frac{h}{2}}\frac{d\bar{z}}{\bar{z}K(\bar{z})} = \int_{R-\frac{h}{2}}^{R}\frac{d\bar{z}}{\bar{z}\left(K_m + K_{cm}\frac{2\bar{z}+h}{h}\right)} + \int_R^{R+\frac{h}{2}}\frac{d\bar{z}}{\bar{z}\left(K_m+K_{cm}\frac{-2\bar{z}+h}{h}\right)}$$

$$I_2 = \int_{R-\frac{h}{2}}^{\bar{z}}\frac{d\zeta}{\zeta K(\zeta)} = \int_{R-\frac{h}{2}}^{R}\frac{d\zeta}{\zeta\left(K_m+K_{cm}\frac{2\zeta+h}{h}\right)} + \int_R^{R+z}\frac{d\zeta}{\zeta\left(K_m+K_{cm}\frac{-2\zeta+h}{h}\right)}$$

in which the details of coefficients $I_i (i = 1, 2)$ as shown in Appendix C.

Substitution of Eq. (36) into Eq. (35) gives temperature distribution across the shell thickness $T(\bar{z})$

$$T(\bar{z}) = T_{m2} + \frac{\Delta T}{I_1}I_2$$

(37)

Replacing Eq. (37) into Eq. (13b) give the thermal parameter Φ_1

$$\Phi_1 = \int_{-\frac{h}{2}}^{0}\left[\left(E_m + E_{cm}\left(\frac{2z+h}{h}\right)\right)\left(\alpha_m + \alpha_{cm}\left(\frac{2z+h}{h}\right)\right)\right]T(z)dz$$
$$+ \int_0^{\frac{h}{2}}\left[\left(E_m + E_{cm}\left(\frac{-2z+h}{h}\right)\right)\left(\alpha_m + \alpha_{cm}\left(\frac{-2z+h}{h}\right)\right)\right]T(z)dz$$

(38)

5. Vibration analysis

Suppose that an ES-S-FGM elliptical cylindrical shells is acted on by a uniformly distributed excited transverse load $p = Q_0 \sin \Omega t$. Substitution of Eq. (32) into (28) leads to:

$$\ddot{\psi}(t) + M_1\psi(t) + M_2(\psi(t) + \psi_0) + M_3\psi(t)(\psi(t) + \psi_0)$$
$$+ M_4\psi(t)(\psi(t) + 2\psi_0)$$
$$+ M_5\psi(t)(\psi(t) + \psi_0)(\psi(t) + 2\psi_0) = M_6Q_0 \sin \Omega t$$

(39)

where the $M_i (i = 1 \div 6)$ - coefficients, are give in Appendix C.

Eq. (39) is the governing equation with temperature-dependent coefficients to study the nonlinear dynamic response of the ES-S-FGM cylindrical shells in thermal environments. The nonlinear dynamic response can be obtained by solving Eq. (39) if the initial conditions are assumed as $\psi(0) = 0$, $\dot{\psi}(0) = 0$ and using the Runge-Kutta method.

In the case for linear free vibration for ES-FGM shells form Eq. (39) obtained as:

$$\ddot{\psi}(t) + (M_1 + M_2)\psi(t) = 0$$

(40)

One can determine the fundamental frequency of natural vibration of the ES-FGM shells as:

$$\omega_L = \sqrt{M_1 + M_2}$$

The equation of nonlinear free vibration of a perfect ES-S-FGM elliptical cylindrical shells is:

$$\ddot{\psi}(t) + (M_1 + M_2)\psi(t) + (M_3 + M_4)\psi^2(t) + M_5\psi^3(t) = 0$$

(41)

The nonlinear vibration frequency of the ES-S-FGM elliptical cylindrical shells,

Seeking solution as $\psi(t) = \xi \cos(\omega t)$ and applying procedure like Galerkin method to Eq. (41) to obtain:

$$\omega_{NL} = \omega_L\left(1 + \frac{8(M_3 + M_4)}{3\pi\omega_L^2}\xi + \frac{3M_5}{4\omega_L^2}\xi^2\right)^{\frac{1}{2}}$$

(42)

where ω_{NL} is the nonlinear vibration frequency and ξ is the amplitude of nonlinear vibration.

6. Numerical result and discussion

The effective material properties $P_r(T)$ in the Eq. (1) is present in Table 1 [6,7,14,32] and the parameters for the ES-S-FGM elliptical cylindrical shells were chosen as below:

Table 2

Effect of volume fraction index on natural frequencies $\omega\,(1/s)$ of FGM cylindrical shells with $R/h = 500$, $L/R = 2$, $(m, n) = (1, 3)$.

N	Ref [6]	Present
0	1120.0512	1114.1815
1	1090.6326	1087.1999
2	1078.9093	1076.9263
5	1065.9689	1065.8955
∞	1051.5722	1054.0197
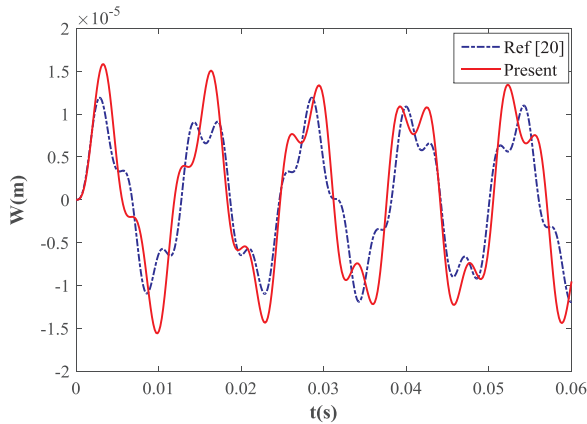
Fig. 4. The comparison of dynamic response of the imperfect S-FGM circular cylindrical shells by CST and by HSDST.

$m = n = 1$, $a/b = 1.5$, $b/h = 100$, $Q_0 = 6000(N/m^2)$, $\Omega = 3000\,(rad/s)$, $\nu = 0.3$,

$$h_x^T = h_y^T = 0.01m, \quad d_x^T = d_y^T = 0.0025m, \quad n_s = 20, \quad n_r = 40, \quad s_x^T = \frac{2\pi R}{n_s},$$

$$s_y^T = \frac{L}{n_s}$$

and assumed that the stiffeners are made by full metal, so $E^s = E_m$, $\alpha^s = \alpha_m$; n_r and n_s are the number of strings, rings of the shells, respectively.

6.1. Validation studies

To validate the reliability of the method used in the paper, the comparisons on dynamic response and vibration are made with results of the study [6,20]. We choose $a = b$, the elliptical cylindrical shells will turn into the circular cylindrical shells.

Table 2 shows a comparison between the present results for the S-FGM shells in the paper and Bich's results for P-FGM shell [6] with the same geometrical parameters. As can be seen, a good agreement is obtained in this comparison.

Fig. 4 indicates the comparison of dynamic response of the imperfect S-FGM shells without elastic foundations with the same geometrical parameters $L/R = 2$, $(m, n) = (1, 1)$, $Q_0 = 6000(N/m^2)$, $N = 1$; $a = b = 40h$. The present using the classical shell theory (CST) and Duc et al. in [20] uses the higher order shear deformation shell theory (HSDST) for the circular S-FGM without elastic foundations. The result shows that the vibration amplitude using the classical shell theory is larger than vibration amplitude using the higher order shear deformation shell theory. This is consistent with conclusions and comparison results in [20] and shows the validity of the obtained results.

6.2. Nonlinear dynamic response

The effect of elastic foundations and pre-loaded axial loads on the

Table 3

Effect of elastic foundations and mechanical loads on natural frequencies $\omega\,(1/s)$ of the ES-FGM elliptical cylindrical shells.

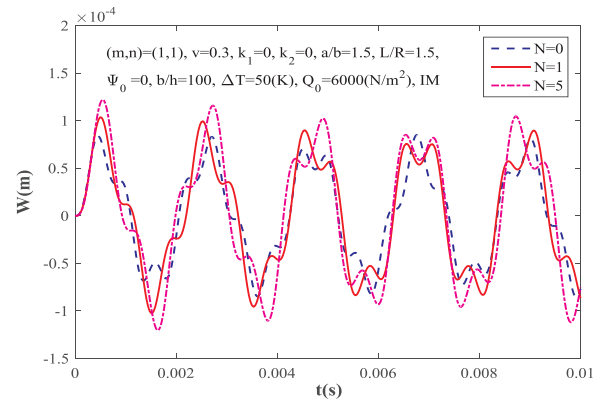|		$k_2 = 0$	$k_2 = 0.02\ GPa.\,m$	$k_2 = 0.04\ GPa.\,m$
$P_x = 0$	$k_1 = 0$	4140	4542	4912
	$k_1 = 1\ GPa/m$	4535	4905	5249
	$k_1 = 2GPa/m$	4898	5242	5566
$P_x = 0.3\ GPa$	$k_1 = 0$	3688	4134	4537
	$k_1 = 1GPa/m$	4126	4529	4900
	$k_1 = 2GPa/m$	4522	4893	5238
$P_x = 0.5\ GPa$	$k_1 = 0$	3352	3838	4269
	$k_1 = 1\ GPa/m$	3829	4261	4652
	$k_1 = 2GPa/m$	4253	4645	5007

Fig. 5. Effects of volume fraction index on the nonlinear dynamic response of the ES-S-FGM elliptical cylindrical shells.
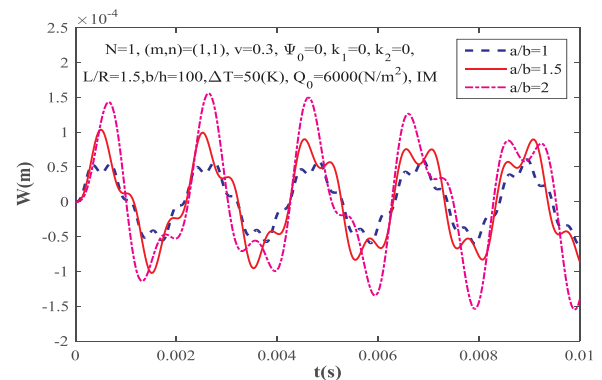

Fig. 6. Effects of ratio a/b on the nonlinear dynamic response of the ES-S-FGM elliptical cylindrical shells.

natural frequency of the ES-FGM elliptical cylindrical shells are shown in Table 3. The value of the natural frequency increases when the values k_1 and k_2 increase and the natural frequency decreases when the value P_x increases. It can be seen that elastic foundations have positive effect whilst P_x has negative effect on the natural frequency value. Furthermore, the Pasternak elastic foundation influences on the natural frequency larger than the Winkler foundation.

Fig. 5 shows the effects of the volume fraction index $N = (0, 1, 5)$ on the nonlinear dynamic response ES-S-FGM elliptical cylindrical shells. As can be seen, the amplitudes of nonlinear vibration of ES-S-FGM shells increase when increasing the volume fraction index N.

Fig. 6 shows the influence of ratio $a/b = (1, 1.5, 2)$ on the nonlinear dynamic response of the ES-S-FGM elliptical cylindrical shells. From Fig. 6, it can be seen that when a/b is increased, the value of the shells amplitude increases and vice versa.

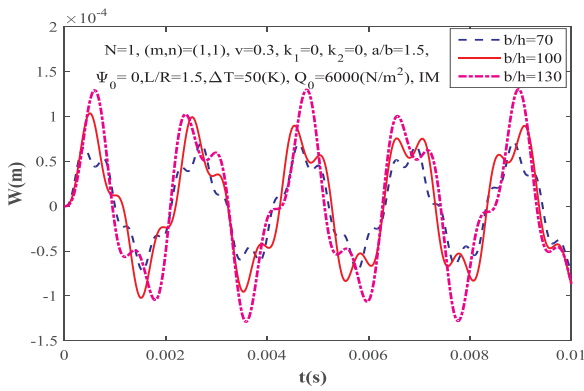Fig. 7 shows the effects of ratio $b/h = (70, 100, 130)$ on the

Fig. 7. Effects of ratio *b/h* on the nonlinear dynamic response of the ES-S-FGM elliptical cylindrical shells.
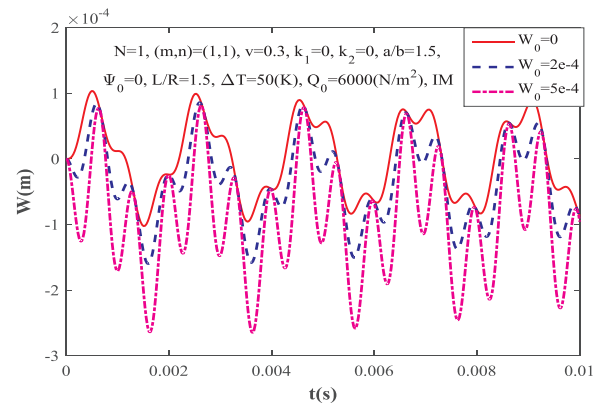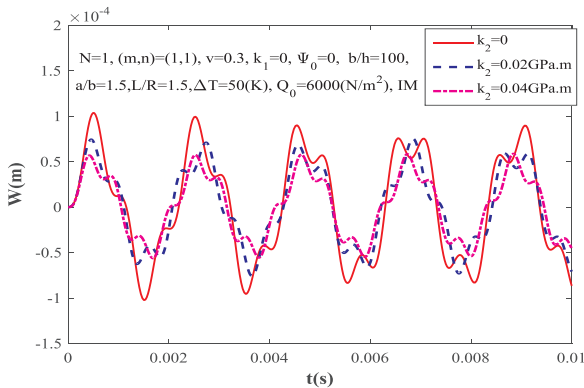

Fig. 8. Effects of the Pasternak foundation on the nonlinear dynamic response of the ES-S-FGM elliptical cylindrical shells.
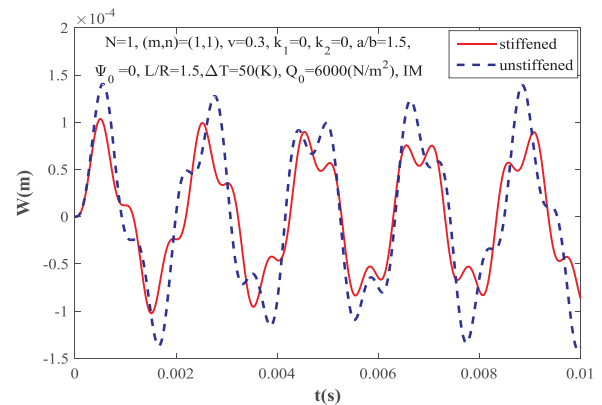

Fig. 9. Effects of the Winkler foundation on the nonlinear dynamic response of the ES-S-FGM elliptical cylindrical shells.

Fig. 10. Effects of imperfection W_0 on the nonlinear dynamic response of the ES-S-FGM elliptical cylindrical shells.

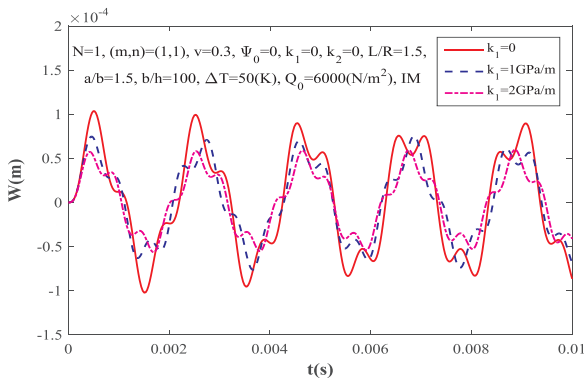**Fig. 11.** Effects of stiffeners on the nonlinear dynamic response of the ES-S-FGM elliptical cylindrical shells.
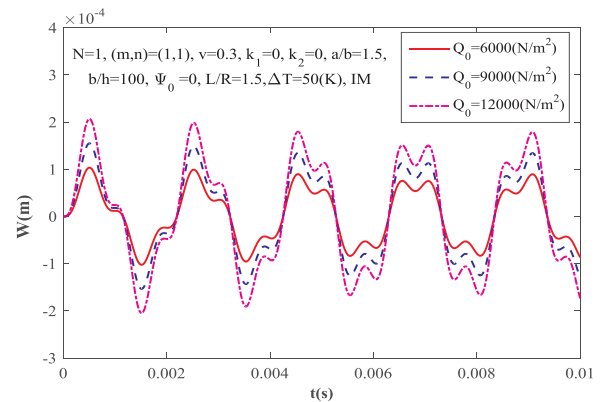

Fig. 12. Effects of amplitude Q_0 on the nonlinear dynamic response of the ES-S-FGM elliptical cylindrical shells.

nonlinear dynamic response of the ES-S-FGM elliptical cylindrical shells. It is obvious that, the higher the ratio *b/h*, the higher the amplitude of the cylindrical shells.

Figs. 8 and 9 consider the effects of coefficients k_1, k_2 of the linear Winkler and Pasternak foundations, respectively, on the nonlinear dynamic response of the ES-FGM elliptical cylindrical shells. From the figures, we can see that the amplitude fluctuation of the shells decreases when the coefficients of elastic foundations increase. Or in other words, the elastic foundations have a positive effect on the reduction of the amplitude fluctuation of the shells. In addition, compared with the case of corresponding to the coefficient k_1 of the Winkler model, the Pasternak type elastic foundation with coefficient k_2 has a stronger effect.

Fig. 10 indicates influence of initial imperfection on nonlinear dynamic response of the ES-S-FGM elliptical cylindrical shells. The

increase imperfection will lead to the increase of the amplitude of maximum deflection.

Fig. 11 shows the effect of eccentrically stiffeners on the nonlinear dynamic response of the ES-S-FGM elliptical cylindrical shells. Clearly, the result shows that the stiffeners strongly decrease vibration amplitude of the S-FGM shells.

The effect of excitation force amplitude $Q_0 = (6000, 9000, 12000)$ on nonlinear dynamic response of the ES-S-FGM elliptical cylindrical shells are shown in Fig. 12. As can be observed, the increase in excitation force amplitude will lead to the increase of the ES-S-FGM nonlinear response amplitudes.

Fig. 13 indicates the dynamic responses of the ES-S-FGM elliptical shells, when the frequency of the exciting force is near to the natural
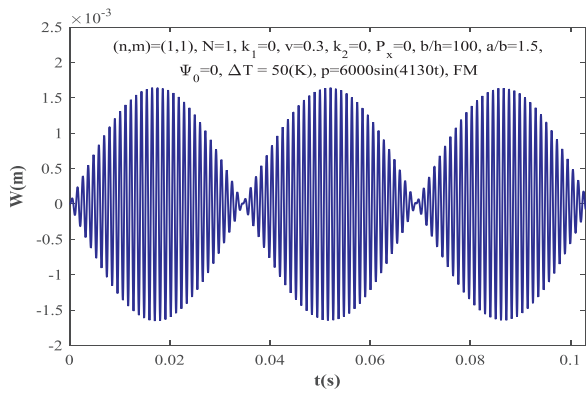
Fig. 13. The harmonic beat phenomenon of the ES-S-FGM elliptical cylindrical shells.
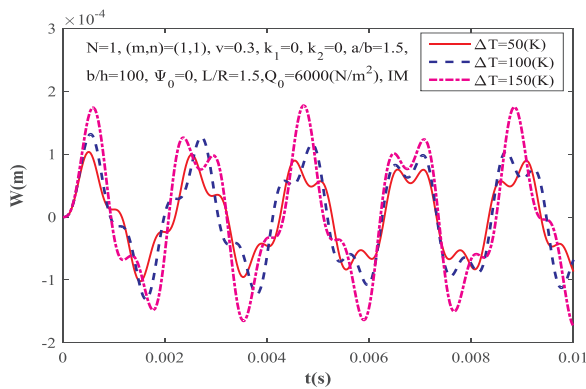

Fig. 14. Effects of temperature on the nonlinear dynamic response of the ES-S-FGM elliptical cylindrical shells.
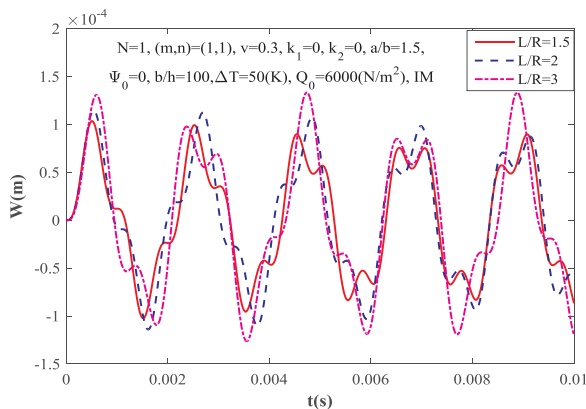

Fig. 15. Effects of ratio L/R on the nonlinear dynamic response of the ES-S-FGM elliptical cylindrical shells.

Fig. 16. The comparison of dynamic response of the ES-S-FGM elliptical cylindrical shells and the ES-FGM circular cylindrical shells in [2].

Fig. 17. Comparison of nonlinear dynamic response of the ES-S-FGM elliptical cylindrical shells in the case of uniform temperature and through the thickness temperature gradient.

Fig. 18. Effect of the elastic foundations on frequency-amplitude curve of the ES-S-FGM elliptical cylindrical shells.

frequency of the shell: the natural frequency of the shell $\omega = 4140(1/s)$ and the external frequency $\Omega = 4130(1/s)$. From obtained results, the interesting phenomenon is observed like the harmonic beat phenomenon of a linear vibration.

Fig. 14 illustrates the effects of temperature increment ΔT on the amplitude-time curves of the nonlinear dynamic response of the ES-S-FGM shells. Three sets of thermal environmental conditions are considered $\Delta T = (50, 100, 150)(K)$. It can be seen that the amplitude will increase when the temperature is increased.

Fig. 15 shows the effects of the ratio thickness L/R on the nonlinear dynamic response of the ES-FGM elliptical cylindrical shells. With three case $L/R = (1.5, 2, 3)$ As our expectation, the amplitude of nonlinear dynamic response of the ES-S-FGM shells decreases when decreasing the ratio L/R.

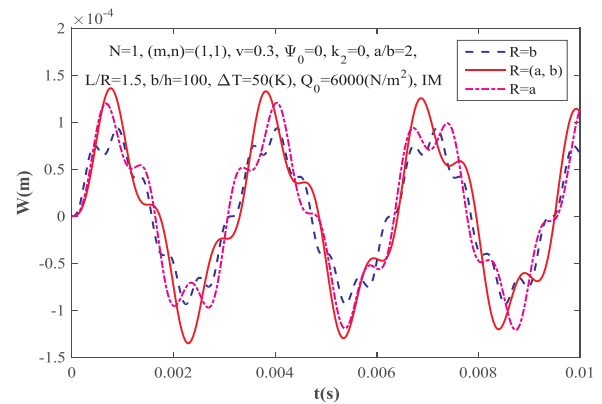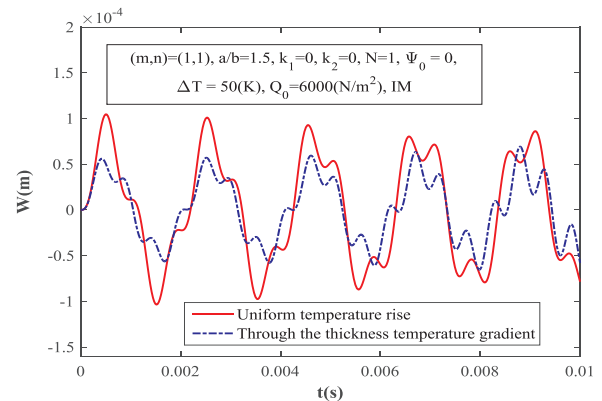Fig. 16 illustrates the comparison of dynamic response of the ES-S-

FGM elliptical cylindrical shells $(R(a, b))$, $(b \leq a)$ and the ES-S-FGM circular cylindrical shells with two cases $R = const = a$ and $R = const = b$ as in [2]. From Fig. 16, we can see that with the same thickness, length and excited transverse load, the present amplitude of ES-S-FGM elliptical cylindrical shells is higher than one of the ES-S-FGM circular cylindrical shells in [2].

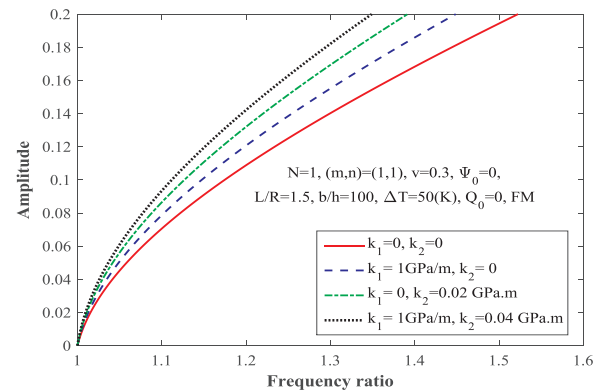Fig. 17 shows the nonlinear dynamic response of the ES-S-FGM elliptical cylindrical shells in the case of uniform temperature and through the thickness temperature gradient, it can be seen that vibration amplitude of the elliptical cylindrical shells in the case of uniform temperature rise is higher. Since then, we can conclude that the load capacity of the shells under the uniform temperature rise is weaker than that one.

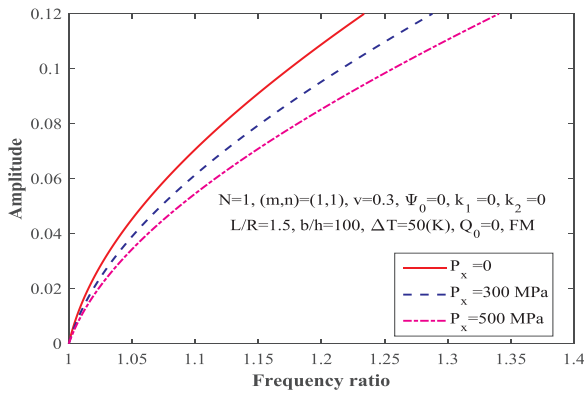The effects of elastic foundations on the frequency-amplitude

Fig. 19. Effect of pre-loaded axial loads on frequency-amplitude curve of the ES-S-FGM elliptical cylindrical shells.

relations of the ES-S-FGM elliptical cylindrical shells present in Fig. 18. It is evident that with the same frequency, ES-S-FGM shells surrounded on elastic foundations have smaller amplitude than the shells without elastic foundations. Furthermore, the Pasternak foundation also has stronger effect on the frequency-amplitude relations of the shells than Winkler foundation.

Fig. 19 presents the effects of pre-loaded axial loads on the frequency-amplitude relations of the nonlinear free vibration of cylindrical shells. Fig. 19 shows that with the same amplitude, when the preloaded increases, the frequency of vibration becomes larger.

7. Conclusion

Some conclusions are obtained from this study:

i. The stiffener system strongly impacts on the dynamic response and vibration of the ES-S-FGM elliptical cylindrical shells. Stringer stiffeners lightly influence while ring stiffeners strongly influence the $t(s) - W(m)$ time–deflection curves of ES-S-FGM shells.

ii. The results obtained also demonstrated that the $t(s) - W(m)$ time–deflection curves were affected greatly by variations in parameters such as the volume fraction index N, the radius-to-thickness ratio b/h, the length-to-radius ratio L/R and ratio a/b

iii. The imperfection, elastic foundations, outside stiffeners and temperature strongly affected the dynamic response and vibration of the ES-S-FGM elliptical cylindrical shells. The amplitude of the shell increases when the temperature and imperfection increase, and the stiffeners and elastic foundations have positive effects on the natural frequency values and amplitudes of the ES-S-FGM shells.

iv. With the same amplitude, when the pre-loaded axial load increases, the frequency of vibration of the ES-S-FGM shells becomes larger.

v. The temperature has significant impact on the nonlinear dynamic response of S-FGM shell. Moreover, the dynamic deflection of the shell in the case of temperature variation through thickness is smaller than one in the case of uniform temperature rise.

vi. The some obtained results are validated by comparing with those in the literature.

vii. Used stress function, Galerkin method, Runge–Kutta method and analytical approach, the nonlinear dynamic responses of the ES-S-FGM eliptical shells are determined by explicit relations of material, geometrical parameters, temperature, outside stiffeners and elastic foundations, so we can actively control dynamic response and vibration of the ES-S-FGM elliptical cylindrical shells by suitable pre-selection of these parameters.

Appendix A

$$A_{11} = \frac{E_1}{1 - v^2} + E^s \frac{A_x^T}{s_x^T}, \quad A_{12} = \frac{E_1 v}{1 - v^2}, \quad A_{22} = \frac{E_1}{1 - v^2} + E^s \frac{A_y^T}{s_y^T}, \quad A_{66} = \frac{E_1}{2(1 + v)},$$

$$B_{11} = \frac{E_2}{1 - v^2} + C_x^T, \quad B_{12} = \frac{E_2 v}{1 - v^2}, \quad B_{22} = \frac{E_2}{1 - v^2} + C_y^T, \quad B_{66} = \frac{E_2}{2(1 + v)},$$

$$D_{11} = \frac{E_3}{1 - v^2} + E^s \frac{I_x^T}{s_x^T}, \quad D_{22} = \frac{E_3}{1 - v^2} + E^s \frac{I_y^T}{s_y^T}, \quad D_{12} = \frac{E_3 v}{1 - v^2}, \quad D_{66} = \frac{E_3}{2(1 + v)},$$

$$E_1 = E_m h + \frac{E_{cm} h}{N + 1}, \quad E_2 = 0, \quad E_3 = \frac{E_m h^3}{12} + \frac{E_{cm} h^3}{2(N + 1)(N + 2)(N + 3)};$$

$$A_x^T = h_x^T d_x^T, \quad z_x^T = \left(\frac{h + h_x^T}{2}\right), \quad C_x^T = \frac{E^s A_x^T z_x^T}{s_x^T}, \quad I_x^T = \frac{d_x^T (h_x^T)^3}{12} + A_x^T (z_x^T)^2$$

$$A_y^T = h_y^T d_y^T, \quad z_y^T = \left(\frac{h + h_y^T}{2}\right), \quad C_y^T = \frac{E^s A_y^T z_y^T}{s_y^T}, \quad I_y^T = \frac{d_y^T (h_y^T)^3}{12} + A_y^T (z_y^T)^2$$

Appendix B

$$h_{11} = -\frac{LR}{4}[C_{11}^* \lambda_m^4 + C_{22}^* \delta_n^4 + (C_{12}^* + C_{21}^* + 4C_{66}^*)\lambda_m^2 \delta_n^2 + k_1 + k_2(\lambda_m^2 + \delta_n^2)] +$$

$$\left[B_{21}^* \lambda_m^4 + B_{12}^* \delta_n^4 + (B_{11}^* + B_{22}^* - 2B_{33}^*)\lambda_m^2 \delta_n^2 - \frac{\lambda_m^2}{R}\right](B_3 - B_4)\left(\frac{LR}{4}\right)$$

$$h_{12} = - \frac{8\lambda_m \delta_n}{3}(B_3 + B_4)$$

$$h_{13} = - \frac{2\lambda_m \delta_n}{3}\left(\frac{B_{21}^*}{A_{11}^*} + \frac{B_{12}^*}{A_{22}^*} - \frac{1}{4R\lambda_m^2 A_{11}^*}\right)$$

$$h_{14} = - \frac{LR}{64}\left(\frac{\lambda_m^4}{A_{22}^*} + \frac{\delta_n^4}{A_{11}^*}\right)$$

Appendix C

$$I_1 = - \frac{1}{K_{cm} + K_m}\left(\begin{array}{l} \ln(4K_{cm}R + K_{cm}h + K_m h) - \ln(4K_{cm}R + K_m h) + \ln(4R - h) \\ + \ln(4K_{cm}R + K_{cm}h - K_m h) - \ln(4R + h) - \ln(4K_{cm}R - K_{cm}h - K_m h) \end{array} \right)$$

$$I_2 = - \frac{1}{K_{cm} + K_m}\left(\begin{array}{l} - \ln(2K_{cm}R + K_m h) - \ln(2) - \ln(2R - h) \\ + \ln(2K_{cm}R + K_{cm}h + 2K_{cm}z - K_m h) - \ln(4R + h) - \ln(z + R) \end{array} \right)$$

$$M_1 = \frac{1}{\rho_1}[C_{11}^*\lambda_m^4 + C_{22}^*\delta_n^4 + (C_{12}^* + C_{21}^* + 4C_{66}^*)\lambda_m^2\delta_n^2 + k_1 + k_2(\lambda_m^2 + \delta_n^2)]$$

$$- \frac{1}{\rho_1}\left[B_{21}^*\lambda_m^4 + B_{12}^*\delta_n^4 + (B_{11}^* + B_{22}^* - 2B_{33}^*)\lambda_m^2\delta_n^2 - \frac{\lambda_m^2}{R}\right](B_3 - B_4)$$

$$M_2 = \frac{\lambda_m^4}{\rho_1}\left(\frac{A_{22}^* - A_{12}^*}{A_{22}^*}\Phi_1 + \Phi_{1x}^s - \frac{A_{12}^*}{A_{22}^*}\Phi_{1y}^s\right), M_3 = \frac{32\lambda_m\delta_n}{3\rho_1 LR}(B_3 + B_4),$$

$$M_4 = \frac{8\lambda_m\delta_n}{3\rho_1 LR}\left(\frac{B_{21}^*}{A_{11}^*} + \frac{B_{12}^*}{A_{22}^*} - \frac{1}{4R\lambda_m^2 A_{11}^*}\right), M_5 = \frac{1}{16\rho_1}\left(\frac{\lambda_m^4}{A_{22}^*} + \frac{\delta_n^4}{A_{11}^*}\right) + \frac{\lambda_m^6}{8A_{22}^*\rho_1}, M_6 = \frac{4}{\lambda_m\delta_n\rho_1}$$

References

[1] G.G. Sheng, X. Wang, Thermal vibration, buckling and dynamic stability of functionally graded cylindrical shells embedded in an elastic medium, J. Reinf. Plast. Compos 27 (2008) (117-34).

[2] N.D. Duc, Nonlinear thermal dynamic analysis of eccentrically stiffened S-FGM circular cylindrical shells surrounded on elastic foundations using the Reddy's third-order shear deformation shell theory, J. Eur. J. Mech. – A/Solids 58 (2016) 10–30.

[3] N.D. Duc, Nonlinear thermo-electro-mechanical dynamic response of shear deformable piezoelectric Sigmoid functionally graded sandwich circular cylindrical shells on elastic foundations, J. Sandw. Struct. Mater. (2016), http://dx.doi.org/10.1177/1099636216653266.

[4] T.Y. Ng, K.Y. Lam, K.M. Liew, J.N. Reddy, Dynamic stability analysis of functionally graded cylindrical shells under periodic axial loading, Int. Solids Struct. 38 (8) (2001) (1295-309).

[5] R. Bahadori, M.M. Najafizadeh, Free vibration analysis of two-dimensional functionally graded axisymmetric cylindrical shell on Winkler–Pasternak elastic foundation by First-order Shear Deformation Theory and using Navier-differential quadrature solution methods, Appl. Math. Model. 39 (2015) 4877–4894.

[6] D.H. Bich, N.X. Nguyen, Nonlinear vibration of functionally graded circular cylindrical shells based on improved Donnell equations, J. Sound Vib. 331 (2012) 5488–5501.

[7] M. Shariyat, Dynamic buckling of suddenly loaded imperfect hybrid FGM cylindrical shells with temperature-dependent material properties under thermo-electro-mechanical loads, Int. J. Mech. Sci. 50 (2008) 1561–1571.

[8] C. Du, Y. Li, X. Jin, Nonlinear forced vibration of functionally graded cylindrical thin shells, Thin-Walled Struct. 78 (2014) 26–36.

[9] A.H. Sofiyev, N. Kuruoglu, Buckling and vibration of shear deformable functionally graded orthotropic cylindrical shells under external pressures, Thin-Walled Struct. 78 (2014) 121–130.

[10] A.H. Sofiyev, N. Kuruoglu, Dynamic instability of three-layered cylindrical shells containing an FGM interlayer, Thin-Walled Struct. 93 (2015) 10–21.

[11] N.D. Duc, P.T. Thang, Nonlinear response of imperfect eccentrically stiffened ceramic-metal-ceramic FGM thin circular cylindrical shells surrounded on elastic foundations and subjected to axial compression, Compos. Struct. 110 (2014) 200–206.

[12] Z.G. Song, L.W. Zhang, K.M. Liew, Active vibration control of CNT-reinforced composite cylindrical shells via piezoelectric patches, Compos. Struct. 158 (2016) 92–100.

[13] H.S. Shen, Nonlinear vibration of shear deformable FGM cylindrical shells surrounded by an elastic medium, Compos. Struct. 94 (2012) 1144–1154.

[14] R. Kandasamy, R. Dimitri, F. Tornabene, Numerical study on the free vibration and thermal buckling behavior of moderately thick functionally graded structures in thermal environments, Compos. Struct. 157 (2016) 207–221.

[15] H.A. Sepiani, A. Rastgoo, F. Ebrahimi, A. Ghorbanpour Arani, Vibration and buckling analysis of two-layered functionally graded cylindrical shell, considering the effects of transverse shear and rotary inertia, Mater. Des. 31 (2010) 1063–1069.

[16] R. Kadoli, N. Ganesan, Buckling and free vibration analysis of functionally graded cylindrical shells subjected to a temperature-specified boundary condition, J. Sound Vib. 289 (2006) 450–480.

[17] H.A. Sepiani, A. Rastgoo, F. Ebrahimi, A. Ghorbanpour Arani, Vibration and buckling analysis of two-layered functionally graded cylindrical shell, considering the effects of transverse shear and rotary inertia, Mater. Des. 31 (2010) 1063–1069.

[18] A.A. Jafari, S.M.R. Khalili, M. Tavakolian, Nonlinear vibration of functionally graded cylindrical shells embedded with a piezoelectric layer, Thin-Walled Struct. 79 (2014) 5–15.

[19] F. Mehralian, Y.T. Beni, R. Ansari, Size dependent buckling analysis of functionally graded piezoelectric cylindrical nanoshell, Compos. Struct. 152 (2016) 45–61.

[20] N.D. Duc, N.D. Tuan, T. Phuong, N.T. Dao, N.T. Dat, Nonlinear dynamic analysis of Sigmoid functionally graded circular cylindrical shells on elastic foundations using third order shear deformation theory in thermal environments, Int. J. Mech. Sci. 101–102 (2015) 338–348.

[21] Z.Q. Yue, H.T. Xiao, L.G. Tham, Elliptical crack normal to functionally graded interface of bonded solids, Theor. Appl. Fract. Mech. 42 (2004) 227–248.

[22] M. Ganapathi, B.P. Patel, H.G. Patel, Free flexural vibration behavior of laminated angle-ply elliptical cylindrical shells, Comput. Struct. 82 (2004) 509–518.

[23] F. Tornabene, N. Fantuzzi, M. Bacciocchi, R. Dimitri, Free vibrations of composite oval and elliptic cylinders by the generalized differential quadrature method, Thin Walled Strict. 97 (2015) 114–129.

[24] F. Tornabene, N. Fantuzzi, M. Bacciocchi, R. Dimitri, Dynamic analysis of thick and thin elliptic shell structures made of laminated composite materials, Compos. Struct. 133 (2015) 278–299.

[25] M. Khalifa, Effects of non-uniform Winkler foundation and non-homogeneity on the free vibration of an orthotropic elliptical cylindrical shell, Eur. J. Mech. 49 (2015) 570–581.

[26] V. Gholizadeh, A. Rostami, Golmohammadi, K. Abbasian, A. Javadi, Non singular material parameters for arbitrarily elliptical-cylindrical invisibility cloaks, Optik 124 (2013) 2174–2179.

[27] T.Y. Li, L. Xiong, X. Zhu, Y.P. Xiong, G.J. Zhang, The prediction of the elastic critical load of submerged elliptical cylindrical shell based on the vibro-acoustic model, Thin-Walled Struct. 84 (2014) 255–262.

[28] S. Shariati, M.M. Rokhi, The numerical and experimental investigations on buckling of steel cylindrical shells with elliptical cutout subject to axial compression, Thin-Walled Struct. 46 (2008) 1251–1261.

[29] M.K. Ahmed, Buckling behavior of a radially loaded corrugated orthotropic thin-elliptic cylindrical shell on an elastic foundation, Thin-Walled Struct. 107 (2016) 90–100.

[30] B.P. Patel, S.S. Gupta, M.S. Loknath, C.P. Kadu, Free vibration analysis of functionally graded elliptical cylindrical shells using higher-order theory, Compos. Struct. 69 (2005) 259–270.

[31] D.G. Zhang, Nonlinear bending analysis of FGM elliptical plates resting on two-

parameter elastic foundations, Appl. Math. Model. 37 (2013) 8292–8309.

[32] N.D. Duc, N.D. Tuan, P. Tran, P.H. Cong, N.D. Nguyen, Nonlinear stability of eccentrically stiffened S-FGM elliptical cylindrical shells in thermal environment, Thin-Walled Struct. 108 (2016) 280–290.

[33] F. Tornabene, N. Fantuzzi, E. Viola, C.R. Batra, Stress and strain recovery for functionally graded free-form and doubly-curved sandwich shells using higher-order equivalent single layer theory, Compos. Struct. 119 (2015) 67–89.

[34] F. Tornabene, N. Fantuzzi, M. Bacciocchi, Free vibrations of free-form doubly-curved shells made of functionally graded materials using higher-order equivalent single layer theories, Compos. Part B Eng. 67 (1) (2014) 490–509.

[35] F. Tornabene, N. Fantuzzi, M. Bacciocchi, M. Viola, J.N. Reddy, A Numerical investigation on the natural frequencies of FGM sandwich shells with variable thickness by the local Generalized Differential quadrature method, Appl. Sci. 7 (2)

(2017) 1–39.

[36] A.S. Volmir, Nonlinear dynamics of plates and shells. Science Edition. Moscow, 1972.

[37] N.D. Duc, Nonlinear dynamic response of imperfect eccentrically stiffened FGM double curved shallow shells on elastic foundation, Compos. Struct. 102 (2013) 306–314.

[38] N.D. Duc, Nonlinear Static and Dynamic Stability of Functionally Graded Plates and Shells, Vietnam National University Press, Hanoi, 2014.

[39] J.N. Reddy, C.D. Chin, Thermomechanical analysis of functionally graded cylinders and plates, J. Therm. Stress 21 (1998) 593–626.

[40] D.D. Brush, B.O. Almroth, Buckling of Bars Plates and Shells, Mc Graw-Hill, New York, 1975.